

Improved Resolution and Sensitivity in ^1H -Detected Heteronuclear Multiple-Bond Correlation Spectroscopy

AD BAX AND DOMINIQUE MARION*

*Laboratory of Chemical Physics, National Institute of Diabetes and Digestive and Kidney Diseases,
National Institutes of Health, Bethesda, Maryland 20892*

Received December 14, 1987; revised February 1, 1988

^1H -detected multiple-bond correlation (HMBC) provides an extremely effective method for long-range ^1H - ^{13}C shift correlation (1). The sequence of this experiment is sketched in Fig. 1. In the most common application, indirect detection of ^{13}C via ^1H , a J filter (2) may be used to reject one-bond correlations that could cause overcrowding of the 2D spectrum (1). The delay Δ_2 following the J filter is needed to generate multiple-bond multiple-quantum coherence. Typically, this delay is set to about 60 ms. The dephasing of the ^1H magnetization caused by homonuclear coupling present during this Δ_2 period causes large phase perturbations in the F_2 dimension and makes the recording of 2D absorption spectra impossible. In principle, z -filtering procedures (3), purging pulses (4, 5), and bilinear rotations (6, 7) could be used to restore absorption-mode character in the ^1H dimension. In practice, however, the z filters and purge pulses seriously decrease sensitivity; bilinear rotations require a substantial number of ^1H pulses and seriously affect the suppression of the much stronger signals from protons not coupled to ^{13}C . Regardless, it appears impossible in practice to devise a generally applicable bilinear rotation that refocuses homonuclear ^1H coupling for protons that have a long-range coupling to a ^{13}C nucleus. Therefore, it was suggested previously to record the experiment in the phase-modulated manner, and to use absolute value mode calculation on the data.

As will be demonstrated here, a more effective way of handling the acquired data is to treat them in the hypercomplex format (8, 9). The data then can be processed to be absorptive in the ^{13}C dimension, followed by an absolute value mode calculation in the ^1H dimension. This approach offers a gain in sensitivity of $\sqrt{2}$ plus a significant improvement in ^{13}C resolution.

The signals acquired in odd- and even-numbered scans of the HMBC experiment (when using the phase-cycling procedure given in the legend to Fig. 1) are stored in separate memory locations. Both sets of detected signals are modulated in phase by the homonuclear J couplings and modulated in amplitude by the offset frequency of the ^{13}C nucleus, Ω_C . In practice, the acquisition time in the t_1 dimension of the 2D experiment is chosen quite short (about 30 ms). The J modulation during this time

* On leave from Centre de Biophysique Moleculaire, Centre National de la Recherche Scientifique, 45071 Orleans Cedex 2, France.

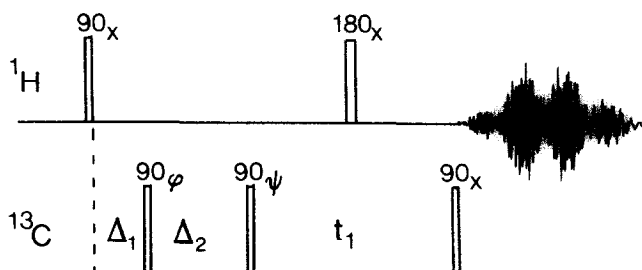


FIG. 1. Pulse scheme of the HMBC experiment. The delay Δ_1 is set to $1/(2J_{\text{CH}})$ and Δ_2 is set to $1/(2^k J_{\text{CH}})$, where J_{CH} is the one-bond and $^k J_{\text{CH}}$ is the long-range ^1H - ^{13}C coupling. To minimize the effects of relaxation, a shorter compromise value of about 60 ms is typically used for Δ_2 . The phase cycling used is $\varphi = x, x, x, x, -x, -x, -x, -x$; $\psi = x, y, -x, -y$; Acq. = $x, x, -x, -x$. Data for odd- and even-numbered scans are stored in separate locations.

will be small and is neglected in the following discussion. Assuming all pulses are infinitely narrow, the odd-numbered scans are modulated by $\cos(\Omega_C t_1)$, the even-numbered scans by $\sin(\Omega_C t_1)$. Addition or subtraction of these two sets of data (after incrementing the phase of the signals of even-numbered scans by 90°) followed by 2D Fourier transformation yields either the coherence transfer echo or the antiecho spectrum (10, 11), also known as n -type or p -type spectra (12). The noise in these two spectra is uncorrelated and it has been proposed previously that reversing the F_1 dimension of one of the two spectra followed by addition to the second spectrum will increase sensitivity (13). This communication demonstrates a more efficient way to treat the data, calculating a spectrum that is absorption mode in the F_1 dimension and absolute value mode in the F_2 dimension. Such mixed-mode representations have been used before, mainly for reasons of convenience (14–16). As mentioned above, pure 2D absorption spectra cannot be obtained in the HMBC experiment and therefore the mixed-mode representation is the best alternative. For completeness, the hypercomplex approach will be briefly discussed below.

The time-domain data formally are described by what is generally referred to as a hypercomplex or four-component signal (17),

$$S(t_1, t_2) = S_{rr}(t_1, t_2) + iS_{ri}(t_1, t_2) + jS_{ir}(t_1, t_2) + jiS_{ii}(t_1, t_2), \quad [1]$$

where i and j are the imaginary units in the t_2 and t_1 dimension, respectively. Hence, every data point in the time domain consists of four components that can be represented by a 2×2 matrix:

$$\mathbf{S}(t_1, t_2) = \begin{bmatrix} S_{rr}(t_1, t_2) & S_{ri}(t_1, t_2) \\ S_{ir}(t_1, t_2) & S_{ii}(t_1, t_2) \end{bmatrix}. \quad [2]$$

The first index refers to t_1 and the second to t_2 . Horizontal pairs in this matrix are the complex data points acquired during t_2 . Thus, in the phase-cycling scheme of Fig. 1, S_{rr} and S_{ri} correspond to the complex data points acquired during the odd-numbered scans. Vertical pairs concern the quadrature detection in the t_1 dimension. Thus, S_{rr} and S_{ir} correspond to the x component of magnetization measured in odd- and even-

numbered scans, respectively. Therefore, if S_{r} is modulated by $\cos(\Omega_{\text{C}}t_1)$, S_{ir} is modulated by $\sin(\Omega_{\text{C}}t_1)$.

Fourier transformation of Eq. [2] with respect to t_2 yields

$$\mathbf{S}(t_1, F_2) = \begin{bmatrix} S_{\text{rc}}(t_1, F_2) & S_{\text{rs}}(t_1, F_2) \\ S_{\text{ic}}(t_1, F_2) & S_{\text{is}}(t_1, F_2) \end{bmatrix}. \quad [3]$$

Subsequent t_1 Fourier transformation gives

$$\mathbf{S}(F_1, F_2) = \begin{bmatrix} S_{\text{cc}}(F_1, F_2) & S_{\text{cs}}(F_1, F_2) \\ S_{\text{sc}}(F_1, F_2) & S_{\text{ss}}(F_1, F_2) \end{bmatrix}. \quad [4]$$

Below, the frequency variables F_1 and F_2 will be omitted from the matrix notation. This process of hypercomplex Fourier transformation, first introduced by Müller and Ernst (8) and States *et al.* (9), now is widely used in 2D NMR (17). As mentioned before, the phase in the F_2 dimension is affected by homonuclear J modulation during the relatively long interval Δ_2 and cannot be restored to absorption in this dimension. If all pulses were δ pulses, the phase of S_{cc} and S_{cs} would be purely absorptive in the F_1 dimension. The finite widths of the ^1H 180° pulse and the ^{13}C 90° pulses cause a frequency-dependent phase shift in the F_1 dimension which may be quite large and can be difficult to adjust interactively. To a good approximation, the 90° pulse can be replaced by a δ pulse followed by a delay of $4\tau_{90^\circ}/2\pi$ ($\approx 0.64\tau_{90^\circ}$). Similarly, the last 90° ^{13}C pulse can be replaced by a δ pulse preceded by a delay of duration $0.64\tau_{90^\circ}$. The first real value of t_1 is therefore equal to $T = \tau_{180^\circ}(^1\text{H}) + 2 \times 0.64\tau_{90^\circ}(^{13}\text{C})$. The linear phase correction needed in the t_1 dimension is therefore $2\pi/T$ per hertz (18). The phase at the center of the spectrum in the F_1 dimension should be zero. Phase adjustment in the F_1 dimension is then described by

$$\mathbf{S}'(F_1, F_2) = \begin{bmatrix} S'_{\text{cc}} & S'_{\text{cs}} \\ S'_{\text{sc}} & S'_{\text{ss}} \end{bmatrix} = \begin{bmatrix} \cos(2\pi F_1/T) & \sin(2\pi F_1/T) \\ -\sin(2\pi F_1/T) & \cos(2\pi F_1/T) \end{bmatrix} \begin{bmatrix} S_{\text{cc}} & S_{\text{cs}} \\ S_{\text{sc}} & S_{\text{ss}} \end{bmatrix}. \quad [5]$$

Instead of calculating the regular magnitude spectrum, defined as

$$S_{\text{mag}} = (S_{\text{cc}}^2 + S_{\text{cs}}^2 + S_{\text{sc}}^2 + S_{\text{ss}}^2)^{1/2}, \quad [6]$$

we propose to calculate the mixed-mode spectrum

$$S_{\text{mm}} = (S_{\text{cc}}'^2 + S_{\text{cs}}'^2)^{1/2}. \quad [7]$$

Figure 2a shows such a mixed-mode spectrum, recorded for the antibiotic desferrioxamine (MW 1192), the structure of which was recently determined by NMR (19). To eliminate the absolute value mode t_1 noise from the contour plot, a "skyline projection" onto the F_2 axis is made of a region in the 2D spectrum where no ^{13}C resonances are present, from 165 to 145 ppm in the spectrum of Fig. 2a. This "skyline projection" is then subtracted from each of the F_2 traces of the 2D matrix, resulting in an improved appearance of the spectrum (Fig. 2b). Of course, the improvement resulting from this type of nonlinear processing is only cosmetic. As is the case for symmetrization of 2D spectra, t_1 -noise subtraction has inherent pitfalls; but unlike symmetrization, it may be impossible to tell whether t_1 -noise subtraction has been

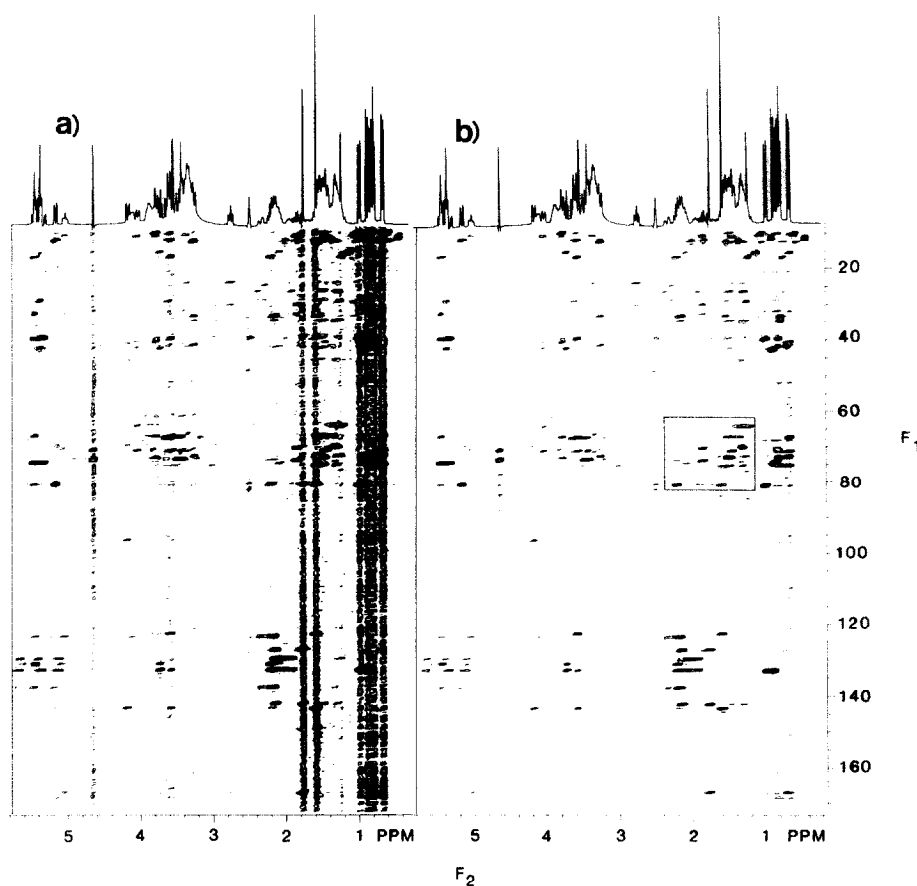


FIG. 2. Mixed-mode (F_1 absorption, F_2 absolute value) HMBC spectra of the antibiotic desertomycin (18), (a) without and (b) with t_1 noise subtraction. The spectrum is recorded at 270 MHz ^1H frequency and results from a $2 \times 330 \times 512$ data matrix. Acquisition times were 27 and 160 ms in the F_1 and F_2 dimension, respectively; 128 scans were recorded per t_1 value and the total measuring time was 13 h. Spectra were recorded using 15 mg of desertomycin (MW 1192) in 0.5 ml $\text{DMSO-}d_6$, at 55°C .

used. Therefore, it is recommended that all published spectra using this type of t_1 -noise subtraction acknowledge this procedure.

The improvement in resolution obtained with this new data processing is demonstrated in Fig. 3, comparing the absolute value mode spectrum and the mixed-mode spectrum for the boxed region of Fig. 2b. Both spectra are derived from the same set of acquired data. In the F_2 dimension, sine-bell multiplication was used for both spectra. For the spectrum of Fig. 3a, 20 Hz Lorentzian line narrowing followed by 40 Hz Gaussian line broadening was used in the t_1 dimension, maximizing F_1 resolution of the absolute value mode spectrum. For Fig. 3b, 25 Hz Gaussian broadening was used to suppress truncation artifacts in the F_1 dimension.

The correlation peaks in Fig. 3a show a skew that is due to phase modulation from ^1H - ^1H J coupling. This skew is not present in the mixed-mode spectrum of Fig. 3b

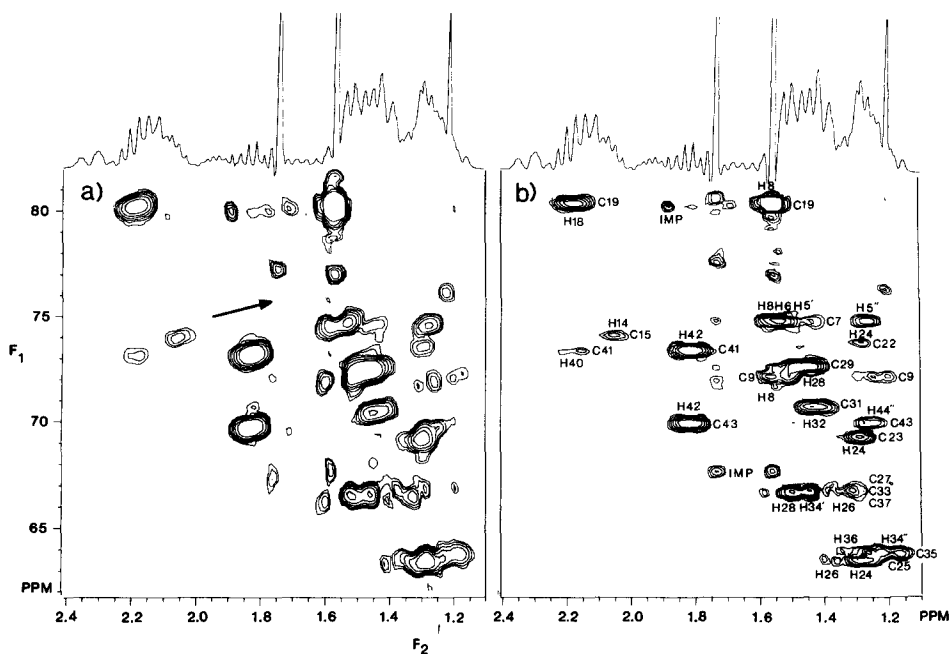


FIG. 3. Comparison of the boxed region of spectrum 2b in (a) the absolute value mode and (b) the mixed-mode representation. The skew of the cross peaks in (a) is indicated with an arrow.

because dispersive data in the F_1 dimension are not used for this spectrum. The phase modulation from homonuclear J coupling is converted into amplitude modulation by eliminating the imaginary part of the data. If the acquisition time in the t_1 dimension is longer than $1/J$, this J modulation will cause a splitting in the F_1 dimension of the cross-correlation multiplet, decreasing F_1 resolution. Hence, the mixed-mode representation can only be used successfully if the acquisition time in the t_1 dimension is short relative to the size of the homonuclear couplings. In practice, the J coupling artifacts are invisible if the t_1 acquisition time is shorter than about 50 ms.

The procedure outlined here yields considerable improvements in sensitivity and resolution of HMBC spectra. One might argue that the increase in F_1 resolution is not real since the mixed-mode approach only works well if a short t_1 acquisition period is used. However, in practice ^1H signals rapidly dephase during increasing t_1 durations because of homonuclear J couplings and hence, for obtaining a high signal-to-noise ratio per unit of measuring time, it is important to restrict the maximum t_1 value. It should be noted that the procedure described here for calculating the F_1 phase is applicable to all phase-sensitive 2D experiments. In our experience, the calculated F_1 phasing is always as good or better than what can be obtained by interactive manual phasing in the F_1 dimension.

ACKNOWLEDGMENTS

D.M. acknowledges financial support from the Centre National de la Recherche Scientifique and from the CNRS-NIH exchange agreement. We thank Rolf Tschudin for continuous technical support.

REFERENCES

1. A. BAX AND M. F. SUMMERS, *J. Am. Chem. Soc.* **108**, 2093 (1986).
2. H. KOGLER, O. W. SØRENSEN, G. BODENHAUSEN, AND R. R. ERNST, *J. Magn. Reson.* **55**, 157 (1983).
3. O. W. SØRENSEN, M. RANCE, AND R. R. ERNST, *J. Magn. Reson.* **56**, 527 (1984).
4. O. W. SØRENSEN AND R. R. ERNST, *J. Magn. Reson.* **51**, 477 (1983).
5. M. H. FREY, G. WAGNER, M. VAŠÁK, O. W. SØRENSEN, D. NEUHAUS, E. WÖRGÖTTER, J. H. R. KÄGI, R. R. ERNST, AND K. WÜTHRICH, *J. Am. Chem. Soc.* **107**, 6847 (1985).
6. J. R. GARBOW, D. P. WEITEKAMP, AND A. PINES, *Chem. Phys. Lett.* **93**, 504 (1982).
7. A. BAX, *J. Magn. Reson.* **52**, 330 (1983).
8. L. MÜLLER AND R. R. ERNST, *Mol. Phys.* **38**, 963 (1979).
9. D. J. STATES, R. A. HABERKORN, AND D. J. RUBEN, *J. Magn. Reson.* **48**, 286 (1982).
10. A. BAX, R. FREEMAN, AND G. A. MORRIS, *J. Magn. Reson.* **42**, 162 (1981).
11. A. BAX, *Bull. Magn. Reson.* **7**, 167 (1986).
12. K. NAGAYAMA, P. BACHMANN, K. WÜTHRICH, AND R. R. ERNST, *J. Magn. Reson.* **40**, 321 (1980).
13. V. SKLENÁŘ AND A. BAX, *J. Magn. Reson.* **71**, 379 (1987).
14. V. SKLENÁŘ, H. MIYASHIRO, G. ZON, H. T. MILES, AND A. BAX, *FEBS Lett.* **208**, 94 (1986).
15. K. NAGAYAMA, *J. Magn. Reson.* **69**, 508 (1986).
16. L. LERNER AND A. BAX, *J. Magn. Reson.* **69**, 375 (1986).
17. R. R. ERNST, G. BODENHAUSEN, AND A. WOKAUN, "Principles of Nuclear Magnetic Resonance in One and Two Dimensions," p. 301, Oxford Univ. Press (Clarendon), London/New York, 1987.
18. In current versions of Bruker software the linear phase correction shown, PHZ1, differs from the correction applied in the F_1 dimension by S11/S12.
19. A. BAX, A. ASZALOS, Z. DINYA, AND K. SUDO, *J. Am. Chem. Soc.* **108**, 8056 (1986).